

Parameter Optimization and Data Fitting for the Flip-Flop Model of Sleep-Wake Regulation

Michal Buiteweg

Abstract

The Levenberg-Marquardt method of parameter optimization is used in an attempt to discover optimized parameters for the physiologically based flip-flop model of sleep-wake developed by Both et al. The model, incorporating an array of physiological processes such as homeostatic sleep drive, circadian rhythm, and macro-scale neurotransmitter activity, aims to model the underlying physiological characteristics of sleep and wake onset. Data from the Entrain application developed by Walch et al. serves as the goal of the optimization: to produce parameters and initial conditions for the flip-flop model that can accurately reproduce data gathered from the application. Methods of converting the Entrain data into useable forms for the optimization are discussed along with the consequences of how choices made about said constructed data influence the quality of parameters and initial conditions found. The quality of found parameters is then discussed along with potential options for improving optimization in the future.

Section 1: Introduction

Overview

Having a mathematical model that accurately predicts human sleep patterns would be a boon for predicting how changes in a person's environment affect their ability to sleep. For instance, such a model could discern how changing the light cycle that an individual is exposed to affects their sleep patterns. It would have the potential to reduce the need for costly and time consuming experiments that require human subjects, and would ultimately allow for a greater understanding of the complex interactions between the sleep drive and the circadian rhythm. This project aims to optimize the parameters of a sleep-wake model developed by Booth et al. to demonstrate its ability to accurately produce sleep patterns based on data collected via research, and to find parameters that can produce a model output that accurately portrays sleep patterns of real data.

Utilizing the flip-flop model of sleep-wake developed by Booth et al. parameter optimization is performed on data of sleep and wake times, as well as light exposure, collected by the Entrain application. Section 2 explores the methods by which optimization was undertaken. Details about the flip-flop model, and the data from the Entrain application are detailed. Section 3 introduces the background information on how the parameter optimization was performed, such as what programming language and optimization method were used. Additionally, this section covers preparation work and includes results of two practice optimizations. Section 4 delivers and discusses the results of the optimization, and details necessary steps for improving results and applying the parameter optimization to more complicated data structures.

Section 2: Methods

The model

The optimization utilized a flip-flop model of sleep-wake cycles developed by Booth et al. [3]. In this model, formalisms attempt to model on a macro scale the levels of neurotransmitters relevant to sleep and wake regulation such as norepinephrine (NE), gamma-aminobutyric acid (GABA), and serotonin (5-HT) [3]. To do this, the model creates a mutually inhibitory, or flip-flop, interaction between the neuronal cluster thought to influence sleep, the ventrolateral preoptic nucleus (VLPO), and the cluster thought to influence wake, the locus coeruleus (LC) [3]. The sleep-wake transitions of the model are driven by the homeostatic sleep drive, with additional influence coming from the circadian rhythm [1].

$$\frac{dH}{dt} = \left\{ \begin{array}{l} \frac{H_{max} - H}{\tau_w} \text{ in wake} \\ \frac{H_{min} - H}{\tau_s} \text{ in sleep} \end{array} \right\}$$

Fig 1. The piecewise differential equation for the homeostatic sleep drive.

The homeostatic sleep drive component of the model is powered by the piecewise equation given in fig 1 [1]. In the model, it acts on the activity of the VLPO, increasing and decreasing its activity when awake or asleep respectively. Current theories about what causes an increase and decrease in

homeostatic sleep drive are inconclusive, but the buildup of adenosine is considered a key suspect in the process [1].

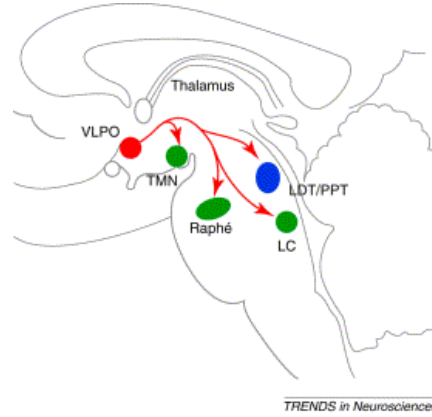


Fig 2. The firing rates of the neuronal clusters in green are collectively referred to as the FLC and the clusters are thought of as one large cluster in the model, whereas the firing rate of the cluster in red is the FVLPO.

A circadian rhythm input was added to the model based on a model developed by Forger et al. [2]. It represents the 24 hour periodic rhythmicity of the circadian clock located in the superchiasmatic nucleus, which modulates activity of the VLPO and the LC. The magnitude of an external light source can be input into the circadian oscillator model, which creates a positive correlation between light exposure and time spent awake.

The neuronal clusters – visualized in fig 2. – are the primary drivers of the model. As the figure notes the model variable FLC actually represents the collective firing rate of several different neuronal clusters. These clusters are not modeled individually, and are instead simplified to just the single firing rate FLC to increase model efficiency with minimal loss of accuracy [3]. In all, the model can be visualized in full in fig 4, and the equations for the model are in fig 3. F represents the firing rate of neurons in Hz, with time in minutes, C the concentration of the neurotransmitters slaved to the LC and VLPO, the parameter $g_{i,x}$ act as a weight for the postsynaptic populations while $\tilde{\tau}_x$ controls the time dynamics of synaptic population firing rate, and $\tilde{\tau}_i$ controls the time dynamics of neurotransmitter expression. Additionally the parameters, α_x , β_x , and γ_x are responsible for slope and half-activation thresholds [3].

$$\frac{dF_x}{dt} = \frac{F_x^\infty \left(\sum_i g_{i,x} c_i(t) \right) - F_x}{\tau_x}, \quad F_x^\infty(c) = \frac{X_{\max}}{2} \left(1 + \tanh \left(\frac{c - \beta_x}{\alpha_x} \right) \right),$$

$$\frac{dc_i}{dt} = \frac{c_i^\infty(F_Y(t)) - c_i}{\tau}, \quad c_i^\infty(f) = \tanh \frac{f}{\gamma}.$$

Fig 3. The general equations used in the model where F is the firing rate of neurons, and C is the concentration of the neurotransmitters relevant to the FLC and VLPO. (Remove bottom left equation)

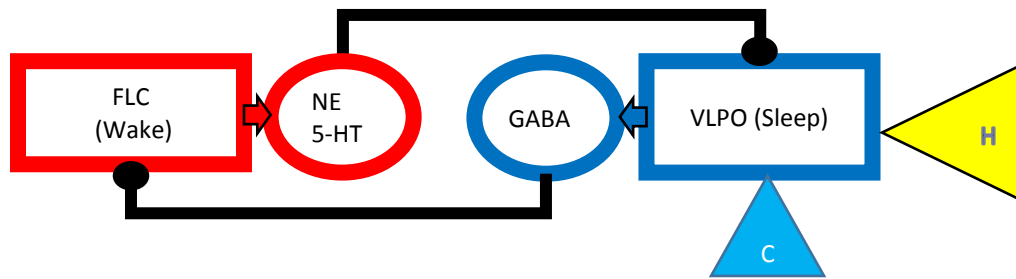


Fig 4. The FLC cluster represents multiple neuronal populations that produce NE, and 5-HT neurotransmitters, which promote wake. The VLPO produces primarily GABA, which promotes sleep. The homeostatic sleep drive and circadian rhythm are accounted for in the model by influencing the VLPO. High homeostatic sleep drive increase VLPO activity, as does low light levels and other factors of the circadian rhythm. The homeostatic sleep drive and circadian rhythm also inhibit VLPO activity during low homeostatic sleep drive, and high light levels.

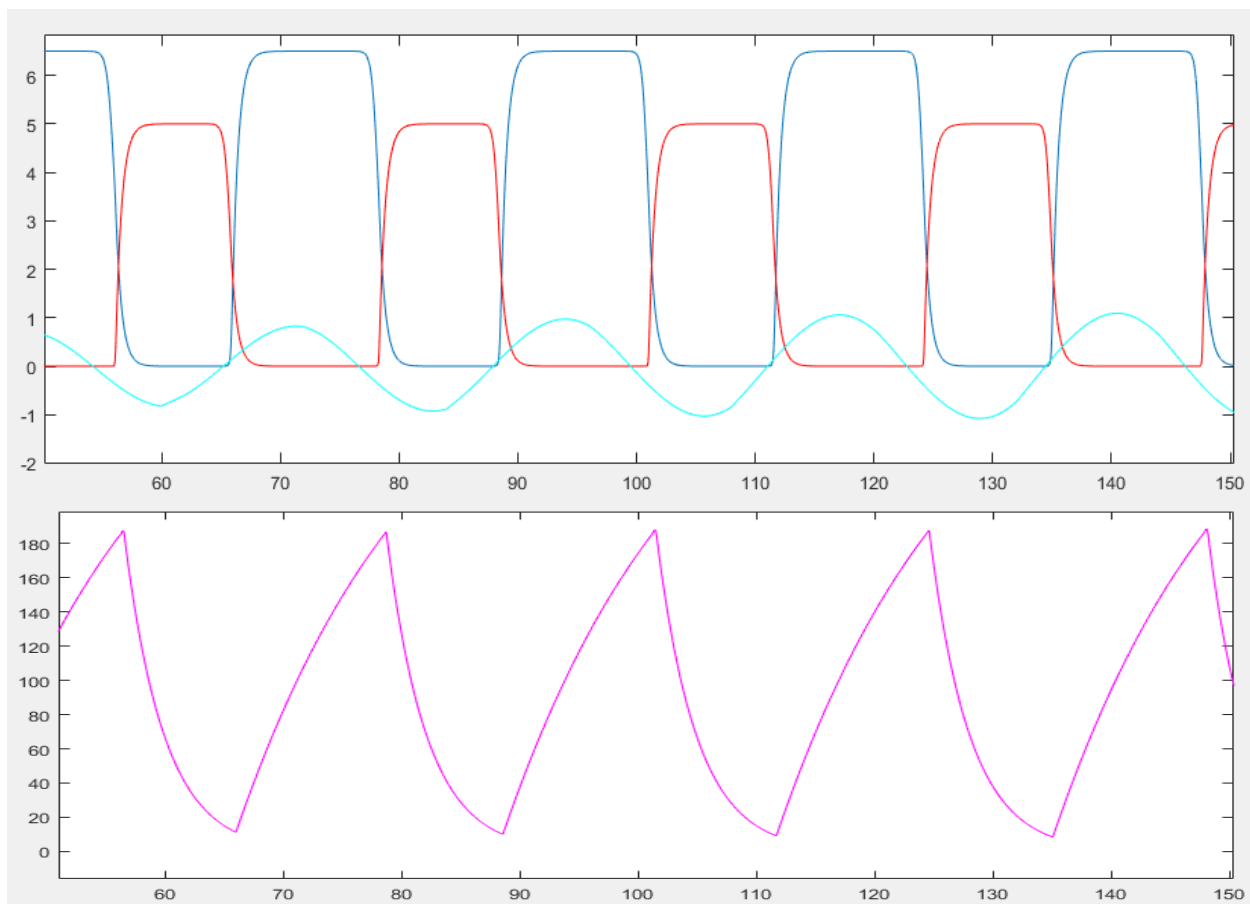


Fig 5. General output from the flip-flop model, where the dark blue line is FLC activity, red is VLPO activity, and the light blue C is the circadian rhythm. The magenta graph is the homeostatic sleep drive. It is easy to note that the sleep drive increase and decreases during wake and sleep to help promote a sleep and wake onset after an extended period of time. Time is in hours.

The data

The data used during optimization was provided by Walch et al. and was gathered using their application Entrain [5]. The application collects user inputted data for sleep times, wake times, and

intensity of sunlight exposure. Of all application users 145 were deemed avid and regular users, and their data was selected for optimization.

Section 3: Background

Optimization Details

The methodology behind parameter optimization is quite vast, and varies wildly between different employable techniques. In general, there exist several iterative processes for parameter optimization that utilize non-linear least squares solving techniques [4].

In general, all methods for solving non-linear least squares problems utilize a least squares equation. This equation measures the distance between observed data and model output, which is then fed into a cost function [4]. The cost function is also universal amongst these methods, and is primarily a means of converting the differences between the model output and observed data into a single value that can then be minimized. A basic and ubiquitous cost function is found in fig 6 where f_i are given functions, in the case of the model they are simply the difference between model output and data. In practice, most software packages compute the residual of the cost function, which is the total difference between all model output points and data points, while only requiring a vector of the distances between model points and data points [4]. This distance is calculated by integrating the model using the Runge-Kutta method with the parameters found on a particular iteration of the optimization method described below. The model output at specific time points is then subtracted from the observed data points and placed in the aforementioned vector.

$$F(x) = \frac{1}{2} \sum_{i=1}^m (f_i(x))^2$$

Fig 6. A basic cost function. In essence, it computes the distance between model output points and data points, squares them, and then sums them together dividing by half.

The goal of all methods for solving non-linear least squares problems is to minimize such a cost function, which translates to finding a global minimum in its topology. As the optimization method being employed iterates through different parameters for the model, the model output will change, which causes the cost function to change at each iteration. This variation of the cost function as a function of model parameter values is what defines the topology of the cost function. Given the difficult topology of many cost functions, the methodology for locating such a global minimum often requires methods more complicated than a simple steepest descent method. One such method is the Levenberg-Marquardt Method, which utilizes parameter dampening using a dampener μ to influence both the direction and size of the change in model parameter values taken towards a minimum [4]. The dampener μ aids in finding a near quadratic final convergence while the process is close to the global minimum and dictating direction and size of the change in the model parameter values to appropriate values when further away from said minimum [4]. The result is a versatile method.

Program

MATLAB R2016a was used for all optimization. The language was chosen for its ease of use and available optimization packages. Other alternatives exist for parameter optimization and data fitting for biological systems, such as the python based sloppy-cell.

Preparation

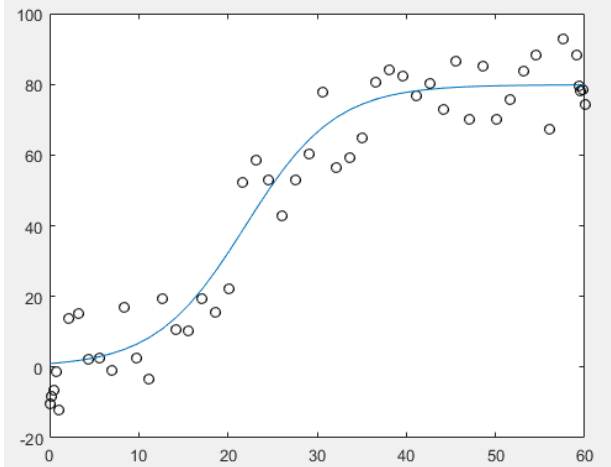
Before attempting to optimize the parameters of the model equations, it was necessary to practice optimization with MATLAB on simpler problems, such as the logistic growth equation and a Van der Pol oscillator. Attempts at optimizing parameters and initial conditions for both were successful, and can be seen in figure 7 and 8.

The logistic growth function only has one initial condition P , population size, and two parameters r , growth rate, and K , carrying capacity. All three were allowed to vary, and the vector of distances passed to the optimization package was calculated using methods described previously. Since the logistic growth model is a non-linear differential equation, the data used in optimization was generated by integration, specifically the use of Runge-Kutta with pre-determined values of $P = 1$, $r = .2$, and $K = 80$. The output of the model with predetermined parameters at specific time points was then randomized using a uniform distribution between -1 and 1.

The logistic model only outputs population size at time t , thus only population size was used to calculate the residual. The Van der Pol oscillator has two initial conditions x and y , as well as one parameter μ , all of which were allowed to vary. The distances used by the cost function are calculated using the data from x and y .

The Van der Pol oscillation was chosen due to the flip-flop model being oscillatory. It proved to be challenging, as the number of generated data points was more important than with a non-oscillating ODE like the logistic equation. If too many data points were generated, the resulting cost function had a topology too rugged for a global minimum to be found, but having multiple oscillations is required for the optimization process to realize it has to create a repeating structure. As such, data points needed to be thinned considerably when generating the random data, but they could only be thinned by removing data points rather than severely truncating the number of oscillations. This accounts for the fewer points in the Van der Pol data set as compared to the logistic growth data set. The data used for optimization was generated in the same fashion as the logistic growth function with values of $\mu = 5.0$, $x = .5683$, and $y = .7917$ and utilizing the same methodology for producing the distance vector.

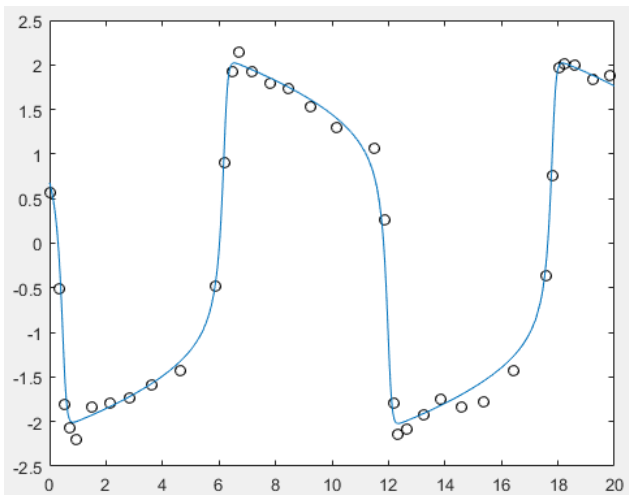
The results, shown in figure 7 and 8, were largely successful. Though not perfect, the found parameters were settling within acceptable ranges from the actual parameters, and – more importantly – the resulting functions matched the shape of the solutions of the actual ODEs quite nicely. Both of these factors gave relative confidence that the optimizations could produce well-fitting parameters. Though it became apparent when optimizing the Van der Pole oscillator that how the data is structured can greatly impact the accuracy of the optimization.



$$\frac{dP}{dt} = rP \cdot \left(1 - \frac{P}{K}\right)$$

Fig 7B. The logistic growth equation

Fig 7A. The output of logistic equation solved using Runge-Kutta with parameters generated by optimization is in light blue, with points representing data randomly generated using a uniform distribution from a logistic growth equation with values $P = 1$, $r = .2$, and $K = 80$. The resulting parameter was $P = .973$, with initial conditions $r = .199$, and $K = 79.87$



$$Z_1 = \mu \left(x - \frac{1}{3} x^3 - y \right)$$

$$Z_2 = \frac{1}{\mu} x$$

Fig 8B. The second order non-linear differential equation for a Van der Pol oscillator reduced to two equations

Fig 8A. The output of a Runge-Kutta numerical solution to a Van der Pole oscillator using parameters and initial conditions located with the Levenberg-Marquardt method of parameter optimization in MATLAB. The found solution is in light blue, and the dots represent data randomly generated with a normal distribution from an oscillator with parameters $\mu = 5.0$, $x = .5683$, and $y = .7917$. The found parameters were $x = .5683$, and $y = .8087$, with initial condition $\mu = 5.0037$.

Section 4: Results

Optimization on Arbitrary Data:

Initially, optimization was conducted on arbitrarily generated data. The model ran with predetermined initial conditions and parameter values detailed in figure 9, then the resulting output at specific time points was randomized using a normal distribution between -1 and 1 just as it was in the

logistic growth model and Van der Pol oscillator. From there the optimization was run in an attempt to yield values that were comparable to these actual parameters and initial conditions. This was done primarily to see what limitations were present with optimization on the model.

The results as shown in fig 9 were quite good, but these tests emphasized the importance of having strong initial guesses for the parameters and initial conditions of the model.

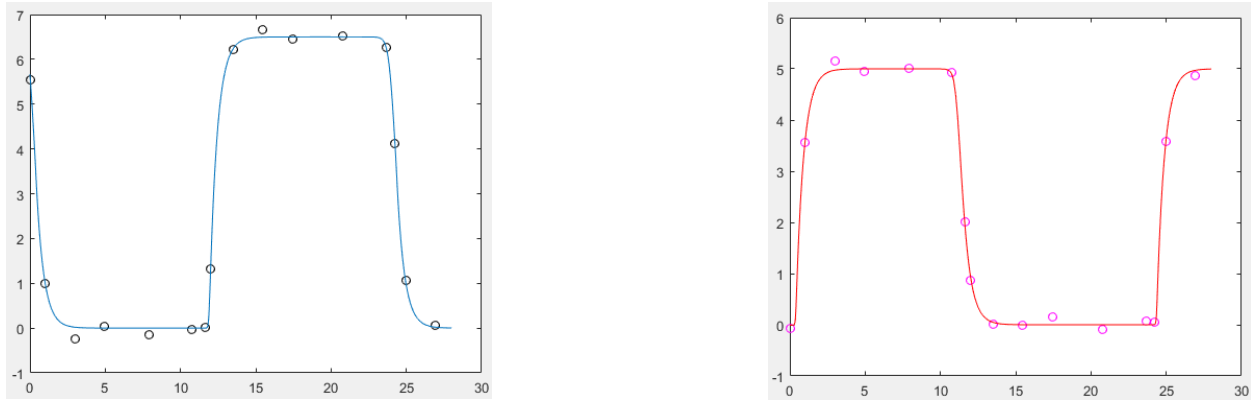


Fig 9. Left: blue is the output FLC from the model run with the found parameters and initial conditions, whereas the dots are the randomized data. Right: red is the output VLPO from the model run with the found parameters and initial conditions, with magenta dots representing the randomized VLPO data points. The real values were $gCircFLC = 1$, $gCircVLPO = -1$, $gGabaLC = 2$, $gNEVLPO = 2$, with initial conditions $FLC = 5.54$, $VLPO = -.078$, and $H = 178.35$. The found parameters were $gCircFLC = .978$, $gCircVLPO = -1.022$, $gGabaLC = 1.95$, $gNEVLPO = 2.028$, with initial conditions $FLC = 5.66$, $VLPO = -.009$, and $H = 178.62$.

The parameters that were allowed to vary in this test were the strengths of the effects of the circadian rhythm on the LC and VLPO, $gCircFLC$ and $gCircVLPO$, respectively, and the strengths of the inhibition between the LC and the VLPO, $gGABALC$ and $gNEVLPO$. The initial conditions for the homeostatic sleep drive, H , the FLC, and the VLPO were all allowed to vary. The vector of residuals was constructed using the method described in section 3 using the original data and model output from the homeostatic sleep drive, the FLC, and the VLPO. Additionally, further information about what these parameters are is detailed in fig 10. With the exception of $gNEVLPO$, which is the parameter responsible for the strength of the effect of the neurotransmitter NE on the VLPO.

Results began to deteriorate in quality as the initial guesses for the parameters and initial conditions were moved further away from the actual values used to generate the data, which revealed the limiting effects of a bad initial guess on optimizations done using the flip-flop model.

Data Construction

Data construction is a crucial part of optimization, as the topology of a cost function is heavily reliant on how the data is constructed. A large portion of any optimization project is producing a data set that is useable with the optimization method. If a data set produces a cost function that is too jagged, the method will become easily trapped in a plethora of local minimums, resulting in inaccurate parameters, and if the data set produces a cost function that is too smooth a similar result occurs.

The parameters and initial conditions used were those most likely to influence optimization in a meaningful way. That is to say parameters of similar function and of minimal consequence were left static. Occasionally adding additional parameters was found to increase the reliability of produced

parameters, but overall it was observed that adding parameters that were redundant from the perspective of optimization did not aid optimization. Additionally, only parameters that had a direct impact on sleep and wake cycles were submitted for optimization and can be seen in fig 10.

Associated component of Model	Variable Name	Status	Description
Ventrolateral preoptic nucleus	gCircVLPO	Parameter	Indicates strength of circadian drive on VLPO.
Locus coeruleus	gCircFLC	Parameter	Indicates strength of circadian drive on LC. Interpreted as activity of cluster
Homeostatic sleep drive	H	Initial Condition	Initial value of the homeostatic sleep drive
Locus coeruleus	FLC	Initial Condition	Initial value of firing rate F, of the LC
Ventrolateral preoptic nucleus	FVLPO	Initial Condition	Initial value of the firing rate F, of the VLPO
Locus coeruleus	gGABALC	Parameter	Interpreted as potency of the neurotransmitter GABA onto the LC
Ventrolateral preoptic nucleus	k1	Parameter	Effect of H on VLPO
Ventrolateral preoptic nucleus	k2	Parameter	Effect of H on VLPO

Fig 10. The various parameters and initial conditions to be optimized in to fit the model to given data.

The parameter for the strength of the effect of neurotransmitter NE, which reflects LC activity and is labelled gNEVLPO, is not included in the optimization as it performs a similar function as the two k parameters.

The optimization required data for FVLPO, FLC, homeostatic sleep drive, and initial conditions for C, XC, and N. C, XC, and N are all associated with the circadian rhythm, and thus completely determined by the external light cycle. For each Entrain dataset, the light cycle was fixed, thus all variables and parameters for the circadian oscillator were not varied in the optimization. All three were generated by running the model with arbitrary parameters and initial conditions and the light cycle generated from the Entrain data until it reached a steady state that was deemed sufficient for providing initial values for them in the model integration

The data from the Entrain application simply indicated whether a user was awake or asleep during a certain hour of the day, and what the intensity of light was during that time [5]. From this a stable sleep period of one wake and one sleep onset per one 24 hour time span was observed. This served as a “normal” sleep-wake cycle for the individual, and was then artificially expanded to a larger time span in accordance with the observed normal sleep-wake cycle. The time span was set up to always begin at a sleep onset for ease of data construction. This data will be referred to as padded data.

The data used in optimization is generated with a time span, the corresponding values of light intensity measured in Lumens, and information on whether the subject is asleep or awake as this is the data provide by the Entrain application [5]. The homeostatic sleep drive is an important part of the optimization, as its unambiguous relationship to FLC and FVLPO activity grants a consistent shape for the

optimization to adhere to. Thus, generating homeostatic sleep drive data is a vital part of the optimization process. Unfortunately the Entrain application has no means of measuring a person's homeostatic sleep drive, thus the data had to be generated. Fortunately homeostatic sleep drive data is relatively easy to construct, by simply using the piece-wise function in fig 1 with the predetermined minimum value for the drive set to 25. The data can then be generated to fit the sleep and wake onset times of the individual by constructing a 24 hour drive. First, the equation for wake homeostatic sleep drive is run beginning at H_{min} and concludes at sleep onset. The final point generated by the wake homeostatic sleep drive equation is used as the starting point for the sleep equation – consequentially making it H_{max} – which is then run for the remaining 24 hours. The dataset for sleep homeostatic sleep drive is set to begin at the start 24 hour cycle due to the time span beginning at sleep onset. The dataset for the wake homeostatic sleep drive is then set to begin the point after the sleep dataset ends. This 24 hour data set is then expanded for the appropriate duration of time.

The FVLPO and FLC data generation only requires the appropriate value for the FVLPO and FLC activity be given during wake and sleep, since both are constant during wake and sleep. However, wake and sleep onsets pose an issue. The entrain data being from hourly records makes it difficult to produce an accurate onset time. The actual construction of the onset is also an issue. During sleep and wake the whole hour can be considered uniform for the purpose of the model, since the version of the model used for optimization does not include REM sleep or fluctuations in the activity of the neuronal clusters during sleep and wake times, thus making FVLPO and FLC activity constant. The onsets, however, occur rapidly due to the flip-flop switch in the model. Since the data is hourly a decision can be made about when in the hour the onset should occur. For ease of data generation the very beginning of the hour was chosen.

A variety of data sets were constructed containing both sparse and dense data. Sparse data contained only one data point per sleep and wake duration, and could have a varying number of points during wake and sleep onset. The use of these sparse data sets is largely influenced by the outcome of the Van der Pol optimization, as well as the flip-flop model optimization with arbitrary, noisy data. If there are fewer points during wake and sleep then their effect on the cost function is lessened, meaning the optimization will prioritize having the correct wake and sleep onsets. Given that the onsets are the only non-constant data points for the FLC and VLPO, it is thought that emphasizing them will aid the optimization in finding parameters that result in model output that fits the shape of the data with greater accuracy. Dense data contained one FLC and VLPO point per hour, with additional points on the onsets.

Optimization of Entrain Data

The optimization with data from the Entrain application attempts to optimize the parameters and initial conditions described in Fig 10.

The addition of the two k parameters – which are both very small – necessitates computing the parameters in log form, so that they cannot change to an improper sign during optimization. The log of all the parameters and the initial conditions of the homeostatic sleep drive, the VLPO, and the FLC is taken and then passed into the cost function, where they are run through the model – except for the initial conditions, which are reverted back from log form – and then used to calculate the distance vector that is fed into the optimization tool. Additionally, all parameters and initial conditions are positive to facilitate the use of non-imaginary logarithms.

Due to the increased uncertainty that was previously mentioned about the location and duration of the sleep and wake onsets, a vector of weights is used to modify the residual. The weight vector is multiplied component wise, meaning that components of the differences vector can be weighted individually. The weight vector is used to represent the uncertainty in the wake and sleep onset points by multiplying them by a number $0 < w \leq 1$. The residuals from the homeostatic sleep drive are also weighted in this manner due to uncertainty about the true value of H_{max} . For the results of the optimization shown later, the weight for the onset point differences was $\frac{1}{2}$, 1 for the homeostatic sleep residuals, and 1 for all FLC and VLPO distances not on an onset.

The lack of a known answer for the parameters and initial conditions creates considerable difficulty for picking good initial values for the optimization. The initial values used for the parameters and variable initial conditions for the first iteration of the Levenberg-Marquardt method have a considerable impact on the method's efficacy. The abundance of local minimums resulting from a jagged topology in the cost function is the primary cause of this phenomena. As such, a variety of initial guesses is required to find one that leads to a local minimum.

To automate the process of locating initial guesses, a simple hill-climb was employed. The hill-climb for this optimization was developed by simply looking at the final residual of the cost function after the Levenberg-Marquardt method had run with a given set of initial guesses. The initial guesses are then randomized along a uniform distribution between -1 and 1, which is then multiplied by an appropriate factor for the expected size of the parameter. The values for the randomization can be seen in fig 11.

Name	Randomness Multiplier	Initial Guess Before Hill-Climb	Initial Guess After Hill-Climb	Optimized Parameter Result
gCircLC	.25	1	1.3124	.6731
gCircVLPO	.25	1	1.320	.3605
gGABALC	.1	.25	.0132	.7139
k1	.1	.1	.1959	.9481
k2	.001	.0025	.0029	0.110
LC Initial Condition	1.1	3	3.2412	1.5044
VLPO initial Condition	1	2.25	2.9369	.02108
H initial Condition	5	140	129.098	162.2645

Fig 11. The parameters and initial conditions being optimized with their initial guesses pre hill-climb, post hill-climb, randomness in the hill-climb, and resulting values from Levenberg-Marquardt method using the post hill-climb initial guesses.

The resulting model output run using the log values of the 5 parameters and the non-log values of the three initial conditions can be seen in fig 12a-c. The overall final residual was 17,351.

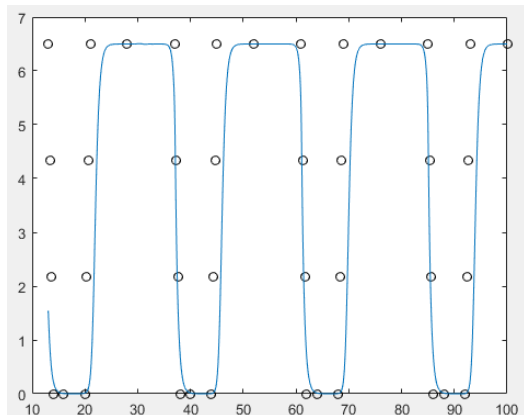


Fig 12a. The FLC model output in light blue against the constructed FLC data in dots.

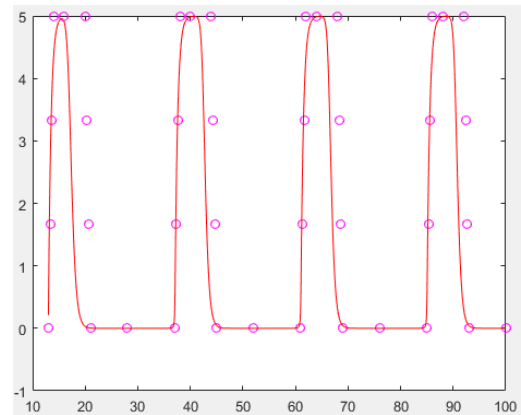


Fig 12b. The VLPO model output in red against the constructed VLPO data in dots.

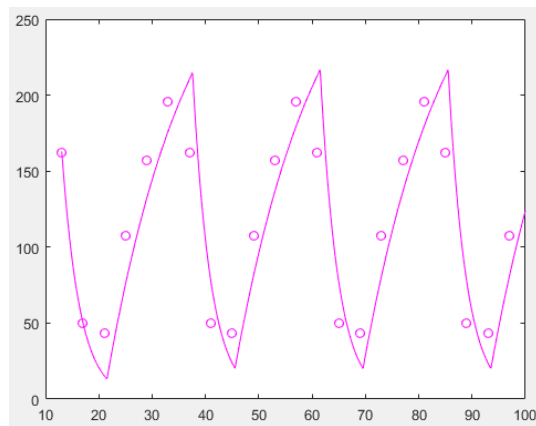


Fig 12c. The homeostatic sleep drive model output in magenta against the constructed homeostatic sleep drive data in dots.

Conclusions and Further Optimization

To discuss the accuracy of the model run using optimized parameters a value of the FLC or VLPO must be established as the point at which the subject is awake or asleep. Since there is no clearly defined point in the model where the subject is considered awake, the point $FLC = 4$ is chosen for being greater than half of the maximum FLC value, but is otherwise arbitrary.

Examining the model after a steady state is achieved reveals that the model output has a wake time spanning from hours 46.1 to 61.13, while the data has a wake time spanning from 44.61 to 61.38. Thus total time awake from model output is 14.97 hours and total time awake from data is 16.77 resulting in a 1.8 hour difference in total wake time. However, a significant portion of this difference is from the difference in onset duration. While the data represents wake and sleep onset with a uniform 1 hour interval, resulting in the onset being from hours 44 to 45, the model onset occurs from approximately hour 44 to 48. Approximate values are used because model output has no clear start and end point, however a change in FLC greater than .1 for the beginning of onset and less than .1 for the

end of onset serves as the measure. The hour 44 to 45 has a change of 0 to .25, and the hour 48 to 49 has a change of 6.41 to 6.47 resulting in a .6 change in the FLC. The differences in the onsets are illustrated in fig 13.

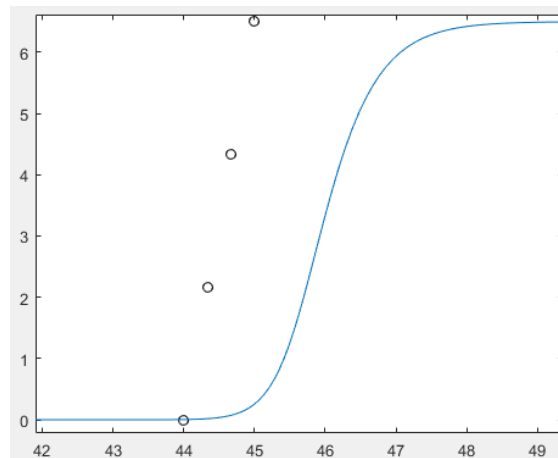


Fig 13. The values of the FLC during a steady state wake onset. The blue line is the model output with optimized parameters, and the black dots are from the constructed data.

With the same criteria as wake onset, the sleep duration has a total discrepancy of 1.55 hours, and the onset occurs between hours 60 and 63 for the model as opposed to the onset occurring between 61 and 62 for the constructed data. These onset durations account for the majority of the error in the model output, and thus reducing the discrepancy of the onset durations is the current priority for further optimization attempts. Potential fixes include constructing the sleep and wake onsets to more accurately match how the model produces them rather than simply having equidistant points over the duration of an hour, adding more data points close to the time when onset begins and ends, and varying the number of total points during the onset.

Final Comments

Given the amount of uncertainty about when during the hour an onset occurs, the model being 1.8 hours off the wake duration and 1.55 off for the sleep duration is an ambiguous result. With the almost unavoidable imperfections in the data construction some error is thought to be inevitable. The question then becomes how much error is acceptable. In all likelihood, a duration error of 1 hour or less is probably ideal due to the onset times occurring anywhere within a one hour range. After achieving a duration of error less than 1 optimizing the non-padded Entrain data is the next step, and proceeding with those optimizations would require a more automatic means of constructing the necessary data for the optimization.

Acknowledgements

Victoria Booth for providing guidance throughout this project and for being part of the development of the flip-flop model of sleep-wake used for optimization.

Kevin Hannay for supplying guidance on optimization methods and techniques.

Olivia Walch for developing the Entrain application and supplying the data collected by it.

The University of Michigan and the REU Program for providing the opportunity to pursue this research.

References

[1] V. Booth, and C.G. Diniz Behn, Physiologically-based Modeling of sleep-wake regulatory networks, *Math Biosci* 250 (2014) 54.

[2] D.B. Forger, M.E. Jewett, R.E. Kronauer, A simple model of the human circadian pacemaker, *J. Biol. Rhythms* 14 (199) 532.

[3] R.D. Gleit, C.G. Diniz Behn, and V. Booth, Modeling Interindividual Differences in Spontaneous Internal Desynchrony Patterns, *J Biol Rhythms* 28 (2013) 339.

[4] K. Madsen, H.B Nielsen, O. Tingleff, *Methods for Non-Linear Least Squares Problems* 2nd Edition, (2004).

[5] O.J. Walch, A. Cochran, and D.B. Forger, A global quantification of “normal” sleep schedules using smartphone data, (2016).